Error Tracking of Radargrammetric DEM from RADARSAT Images

Thierry TOUTIN
Canada Centre for Remote Sensing
588, Booth Street, Ottawa, Ontario, Canada, K1A 0Y7
Tel: (613) 947-1293
Fax: (613) 947-1385
Email: thierry.toutin@ccrs.nrcan.gc.ca

ABSTRACT

In the 1960's, stereoscopic methods were first applied to radar images to derive ground elevation. Unfortunately, research uncovered contradictions between error propagation theory and practical results. These contradictions combined with the lack of stereo radar pairs led to the decline of radargrammetry. The launch in 1995 of Canada's first earth observation satellite, RADARSAT with its various operating modes and specific geometric characteristics has turned the tide. The error propagation of the radargrammetric DEM generated from different RADARSAT stereo configurations is then quantitatively evaluated along the full processing chain (stereo model set-up with ground control points (GCPs), image matching and three-dimensional (3D) intersection). Two matching algorithms are used: automatic and computer-assisted visual matching.

The GCP collection method using stereoscopic plotting is a requisite to achieve the best results for the stereo model and DEM. The automatic matching gives slightly better results than the computer-assisted visual matching, except when the radiometric disparities in the stereo images are too large. Since the geometric advantage (not involved in the automatic matching) can compensate for the radiometric disadvantage, visual matching, which combines both aspects, is a better method in these conditions. Consequently, these two algorithms can be used in a two-step method to generate the best DEM whatever the stereo configuration. Since the relief is an important parameter in the final accuracy, geometric versus radiometric disparity tradeoffs and general guidelines are suggested for selecting RADARSAT stereo pairs for DEM generation as a function of terrain relief.

I INTRODUCTION

In the 1960's, stereoscopic methods [1] were first applied to radar images to derive ground elevation leading to the development of radargrammetry. Unfortunately, research uncovered contradictions and a dichotomy between error propagation theory and practical results, particularly over high relief areas [2]. These contradictions combined with the lack of stereo radar pairs led to the relative decline of radargrammetry.

During the last 20 years, only a few experiments have been realized using satellite images: from the shuttle SIR-B mission over Mt Shasta, USA [3[, [4] and more recently from ERS using the "Roll Tilt Mode" with 23º and 35º incidence angles [5], or using

opposite-side images acquired from ascending and descending orbits [6]. Comparisons of these two research results [7] showed elevation extraction accuracies less than one synthetic aperture radar (SAR) resolution cell (20 m) for the opposite side stereo configuration versus more than one SAR resolution cell (40 m) for the same side stereo configuration. However, stereo configurations were quite limited to address the previously mentioned dichotomy and contradictions.

The launch in 1995 of Canada's first earth observation satellite, RADARSAT with the various operating modes of the SAR and its specific geometric characteristic [8] has turned the tide. In fact, it is the first commercial radar system from which true stereoscopic images and various stereo configurations can be generated from its wide range of incidence angles (from 10º to 60º).

Digital Elevation Model (DEM) generation from stereo SAR images has once more become a hot R&D topic. However, stereoscopy using SAR data is more problematic than visible-and-infrared (VIR) stereoscopy, which emulates human stereo vision. An *a priori* understanding of the physical components of stereo SAR is a prerequisite to resolve the previously mentioned contradictions before any processing and information extraction, and especially DEM generation, can take place.

Preliminary results of generating DEM form RADARSAT-SAR stereoscopic images shown that there was general consensus in the accuracy results [9]: a little more than one resolution for the fine mode (12 m), and little better for the standard mode (20 m). However, there was no significant correlation between the DEM accuracy and the intersection angle and few consensuses on the choice of the best stereo pair.

To expand on these preliminary studies and to better understand RADARSAT-SAR in stereoscopy, the objectives of the paper are first to track the error propagation during the different processing steps of the DEM generation. It thus evaluates various RADARSAT stereo-configurations and the accuracy of the stereo extracted DEM as a function of different geometric and radiometric parameters. Using a SAR parametric solution already developed and tested at the Canada Centre for Remote Sensing (CCRS) [6], ported into a digital stereo workstation, the DVP, and a digital image analysis system, PCI, the processing errors are analyzed, quantitatively evaluated and compared to theoretical prediction. Geometric versus radiometric disparity tradeoffs and general guidelines for selecting RADARSAT stereo-pairs are finally suggested as a function of the results.

II BACKGROUND

Numerous research studies have assessed stereo-capabilities of radar for DEM generation: first with simulated data [10]-[12] due to the lack of a wide range of radar data to generate different stereo-configurations, and then with satellite (SIR, ERS, JERS) data [3]-[6], [13] and many others. The more interesting results to date can be summarized as follows:

1. Reference [10] found that the optimum intersection angles are about 40°- 45°.
2. Reference [11] showed that the best subjective impressions were obtained with shallow look angles (50-70°), and at an intersection angle of 20°.
3. Reference [3] showed that the highest accuracy is not necessarily achieved with the largest intersection angles.
4. Reference [14] noted that higher ground resolution does not necessarily lead to higher height accuracy.
5. Better results are more consistently achieved with opposite-side stereo viewing [6], [14].

These reported results are inconsistent and practical experiments do not clearly support theoretical expectations. For example, larger intersection angles and higher spatial resolution do not translate into higher accuracy. In various experiments, accuracy trends even reverse, especially for rough topography. Only in the extreme case of low relief, does accuracy approach theoretical expectations.

By analogy with photogrammetry, theoretical error analysis were first developed by [15], [16]. They related an error of an exterior orientation element in the left and right images to the resulting error in the stereo-model. These first analyses were mainly limited to absolute errors, and comparing same-side with opposite-side stereo. Reference [17] had a more general approach for the error propagation, identifying both relative and absolute errors irrespective of the stereo configuration. As a summary of the theoretical error propagation modeling, an estimation of the error in the elevation and across-track coordinates, E_h and E_x respectively, due to an error in range, E_r, for the measurement of a target in the stereo image is given by [17]:

$$E_h = [(\sin^2\theta_L + \sin^2\theta_R)^{1/2} / \sin\Delta\theta]\, E_r \quad (1)$$
$$E_x = [(\cos^2\theta_L + \cos^2\theta_R)^{1/2} / \sin\Delta\theta]\, E_r \quad (2)$$

Where θ_L and θ_R are the look angle of the left and right images respectively, and $\Delta\theta$ is the intersection angle as the difference between the two look angles.

As shown in (1) and (2), the errors modeling accounts only for SAR geometric aspects (look and intersection angles, range error) and completely neglects the radiometric aspects (SAR backscatter) of the stereo pair and of the relief. Since SAR backscatter and consequently the image radiometry is much more sensitive to the incidence angle than the VIR reflectance, especially at low incidence angles [18], it generates large radiometric differences between the two images. The theoretical error propagation has thus a major limitation as a tool for predicting accuracy and selecting appropriate SAR stereo images for DEM generation. Care must therefore be taken in attempting to apply VIR stereo concepts to SAR.

One solution to decrease the elevation error E_h is to increase the intersection angle $\Delta\theta$ (1). In other words, to obtain good stereo geometry for better plotting, the intersection angle should be large in order to increase the stereo exaggeration factor or, equivalently,

the observed parallax (large geometric disparities), which is used to determine the terrain elevation (Fig. 1). However, the SAR incidence angle sensitivity will thus generate large radiometric disparities between the images. Conversely, optimum stereo viewing or matching requires a stereo pair as nearly identical as possible (small radiometric disparities), this in turn implies a small intersection angle, which thus reduces the geometric disparities.

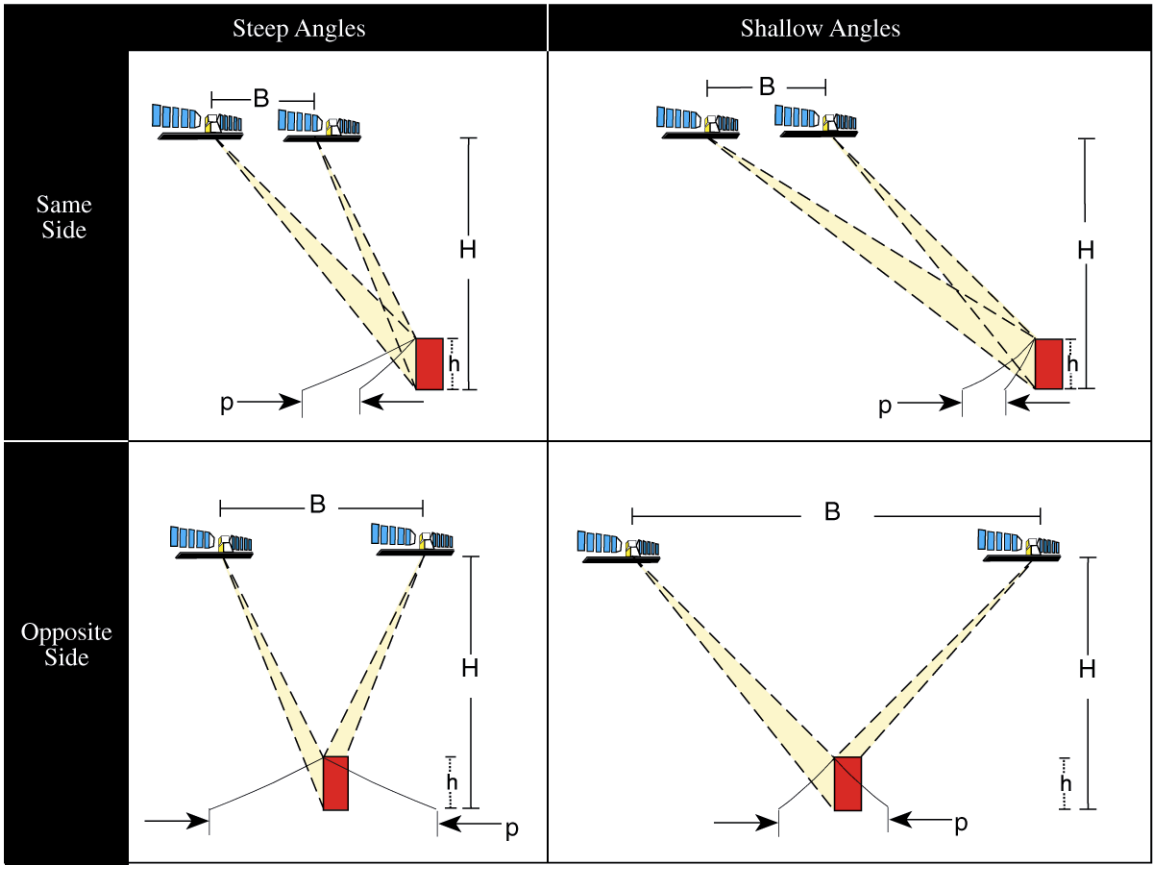

Figure 1: Various configurations of RADARSAT-SAR stereo pairs (same and opposite sides; steep and shallow look angles).

Large geometric and radiometric disparities both hinder stereo viewing and precise stereo plotting. Since the reduction of one disparity could compensate for the other disparity, a tradeoff (steep or shallow look angles, small or large intersection angle, fine or coarse resolution) has to be reached between better stereo viewing (small radiometric differences) and stronger stereo geometry and plotting (large parallax) (Fig. 1).

In general, the tradeoff for any type of relief is to use a same-side stereo-pair, thus reducing both disparities. Unfortunately, this does not maximize the full potential of stereo radar for all topography. The tradeoff between minimizing the radiometric

disparities and maximizing the geometric disparities must take into account the terrain and its relief. For example, opposite-side stereo pairs (large parallax or geometric disparities) should only be used with gentle relief, which reduces the radiometric differences [6]. In some cases the end users should also consider the thematic application and its objectives, such as the image content, the type and level of information to be extracted, and the preferred DEM characteristics.

Since there is an apparent contradiction between the theoretical prediction and the practical experiments for the final DEM error, it is important to track the error during the three main processing steps:

1. The computation of the relative and absolute orientation of the stereo model with Ground Control Points (GCPs), which is a geometric issue;
2. The image matching to find corresponding points in the stereo model, which is a radiometric issue;
3. The stereo intersection to compute the cartographic co-ordinates, which is a geometric issue.

An extra advantage of the error tracking when compared to the computation of the final DEM error is that one can follow and control the error propagation as a function of the input data and the desired accuracy.

III RADARSAT FOR STEREOSCOPY

Historically, the assessment of different radar stereo viewing strategies was impeded by a lack of suitable stereo data sets. Before RADARSAT, no satellite, and only a few airborne radar systems provided data over a broad range of viewing geometry for which this tradeoff could be quantitatively analyzed. RADARSAT (Fig. 2), which acquires imagery from a broad range of look directions, beam positions and modes at different resolutions meets this need.

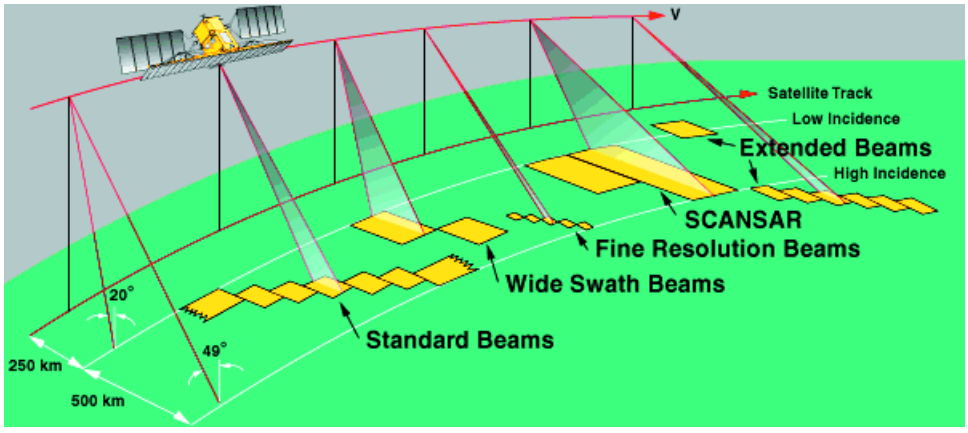

Figure 2: Operating modes of RADARSAT-SAR.

As a result, researchers at CCRS have undertaken an exhaustive study under the Applications Development and Research Opportunity (ADRO) program sponsored by the Canadian Space Agency to evaluate the parameters, which enable a quantitative understanding of radar stereoscopic applications.

Twelve RADARSAT images of the Sherbrooke region, Quebec, Canada were acquired. The relief of the region is moderate with a 450-m elevation range and up-to-30° slopes (Fig. 3). The image data set includes:

1. Four fine mode scenes, 6.25-m pixel spacing, ascending orbit (F1 and F5) and descending orbit (F2 and F4) (Fig. 4); and
2. Eight standard or extended mode scenes, 12.5-m pixel spacing, descending orbit (S1, S4, S7, H3 and H6) (Fig. 5) and ascending orbit (S2, S5 and S7).

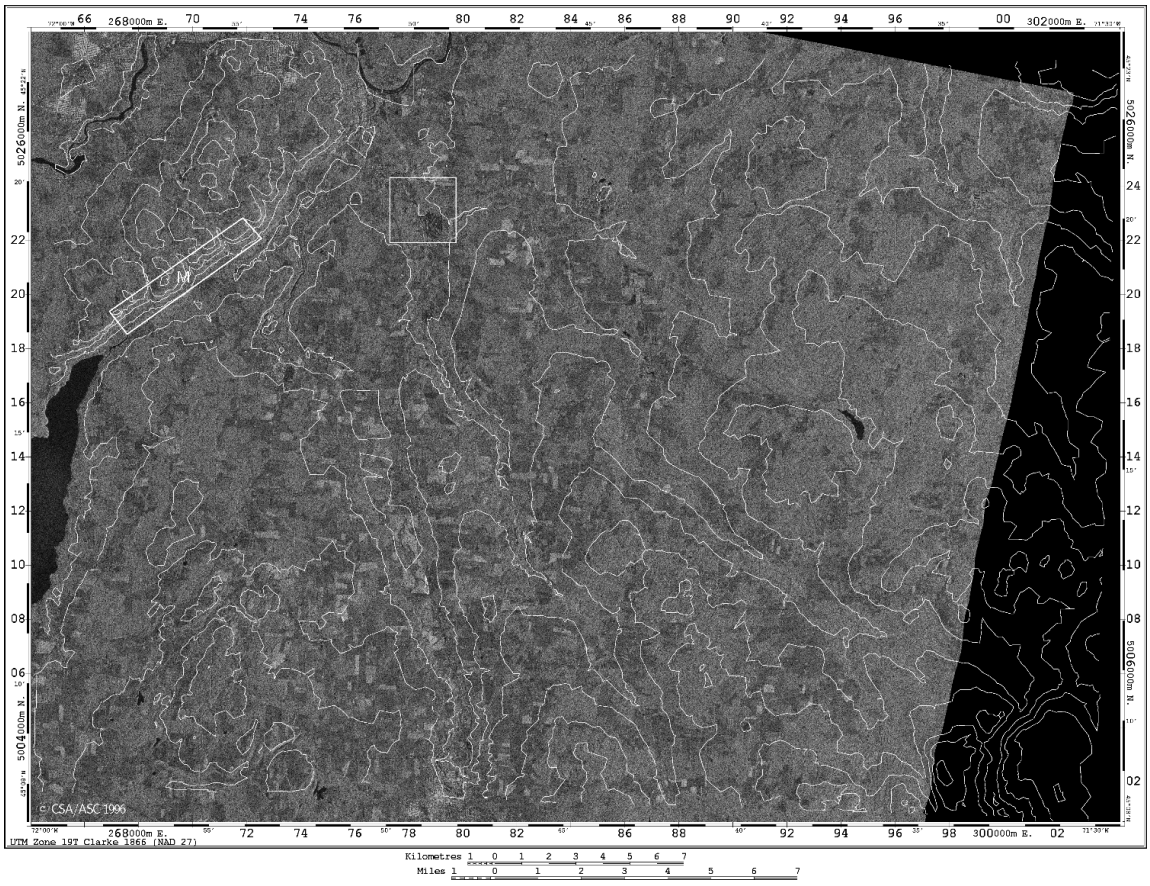

Figure 3: Study site of the Sherbrooke region, Quebec, Canada. Only the 50-m contour lines of the 1:50 000 topographic maps are overlaid in the RADARSAT fine mode SAR ortho-image. The boxes, L and M, are the low and moderate relief areas, respectively. The RADARSAT image is a courtesy of the Canadian Space Agency under the ADRO program.

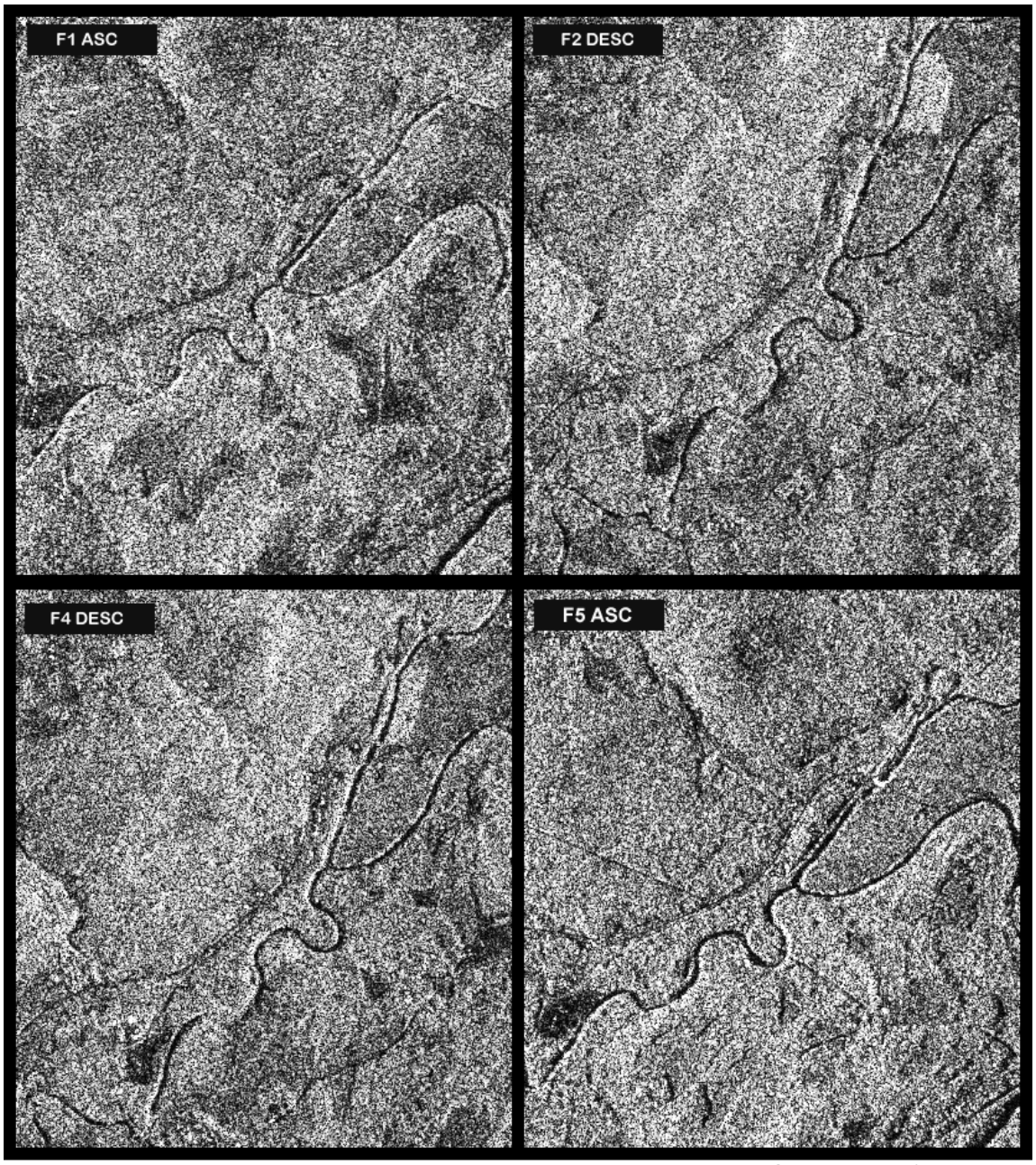

Figure 4: Examples of a sub-area (4 by 4 km) of the fine mode RADARSAT images acquired from ascending (F1, F5) and descending (F2, F4) orbits. RADARSAT images © CSA/ASC 1996.

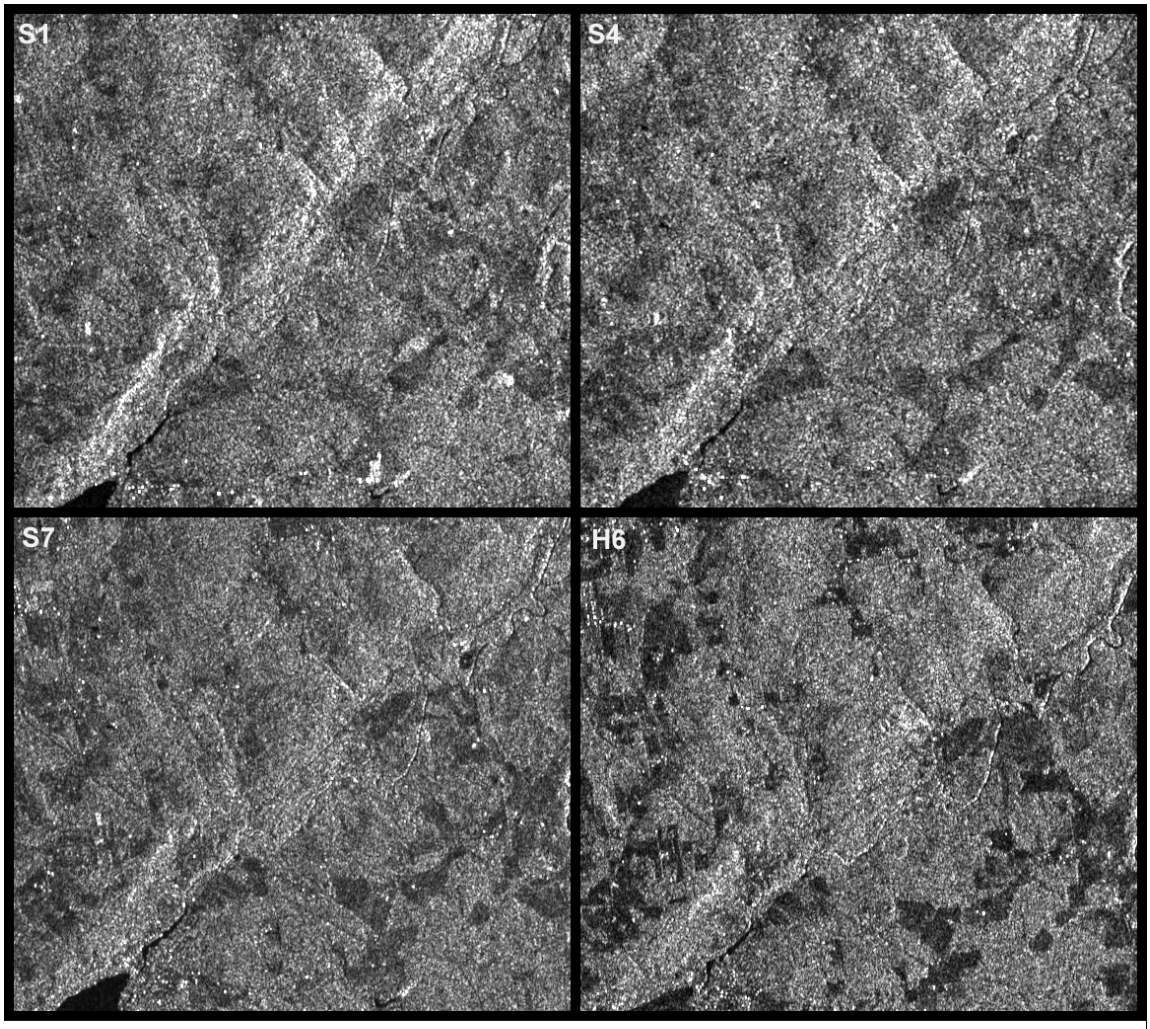

Figure 5: Examples of a sub-area (7 by 6 km) of the standard/extended mode RADARSAT images acquired from descending orbits. The moderate relief test site is along the northern cliff (bottom-left to top-right) of the Massawipi River. Note the effect of look angles on the SAR signal return for this cliff (foreshortening) and for the vegetation fields and forest areas. RADARSAT images © CSA/ASC 1996-1997.

Table I summarizes the general characteristics of the images. They are a good representative set of the most used RADARSAT images: ascending (asc.) and descending (desc.) orbits, various modes (fine, standard, extended), beams and look angles (20º to 60º). The images are in ground range presentation (ellipsoid projection without relief correction), orbit oriented, coded in 16 bits without any radiometric processing. Nine different stereo configurations have thus been generated and studied in detail: fine or coarse resolution, small to large intersection angle (8º to 89º) with steep or shallow look angles, with or without speckle filtering (for the fine mode).

Table I: General characteristics of the RADARSAT images data set.

Mode and Beam	Acquisition Date	Orbit	Look Angle (degrees)	Ground Coverage (km)	Ground Resolution (m)	Pixel Spacing (m)
Fin F1	20/10/96	Asc.	37° - 40°	50 x 50	9.1 x 8.4	6.25 x 6.25
Fin F2	21/10/96	Desc.	39° - 42°	50 x 50	8.7 x 8.4	6.25 x 6.25
Fin F4	04/10/96	Desc.	43° - 46°	50 x 50	8.1 x 8.4	6.25 x 6.25
Fin F5	08/06/96	Asc.	45° - 48°	50 x 50	7.8 x 8.4	6.25 x 6.25
Standard S1	24/10/96	Desc.	20° - 27°	100 x 100	26 x 27	12.5 x 12.5
Standard S2	03/11/96	Asc.	24° - 31°	100 x 100	22 x 27	12.5 x 12.5
Standard S4	14/10/96	Desc.	34° - 40°	100 x 100	25.7 x 27	12.5 x 12.5
Standard S5	24/05/97	Asc.	36° - 42°	100 x 100	24.2 x 27	12.5 x 12.5
Standard S7	10/05/97	Asc.	45° - 49°	100 x 100	20.1 x 27	12.5 x 12.5
Standard S7	22/10/96	Desc.	45° - 49°	100 x 100	20.1 x 27	12.5 x 12.5
Extended H3	04/04/97	Desc.	52° - 55°	75 x 75	19.1 x 27	12.5 x 12.5
Extended H6	12/01/97	Desc.	57° - 59°	75 x 75	18.0 x 27	12.5 x 12.5

By analogy with photogrammetry, the criterion used to analyze a stereo configuration and its potential elevation accuracy is the intersection angle ($\Delta\theta$) or its equivalent base-to-height ratio (B/H) [16], [17]. However, Fig. 1 illustrates that:

1. For same side stereo, the same $\Delta\theta$ or B/H generates a larger elevation parallax with steep look angles than with shallow look angles; and
2. For opposite side stereo, a small $\Delta\theta$ or B/H with steep look angles generates a larger elevation parallax than a large $\Delta\theta$ or B/H with shallow look angles.

It is thus the reverse of VIR stereo images. In fact, the elevation parallax with SAR ground range stereo images can be approximated by [16], [17]:

$$p = h\,[\cot\theta_R - \cot\theta_L] \qquad (3)$$

Where p is the elevation parallax and h the elevation of the target.

The vertical parallax ratio (VPR) p/h seems then to be a better criterion with SAR stereo images than the traditional intersection angle $\Delta\theta$ or base-to-height ratio B/H used with VIR stereo images (Table II).

IV EXPERIMENT

The main processing steps for DEM generation are (i) the stereo model set-up and (ii) the data extraction or capture by image matching and (iii) the three-dimensional (3D) stereo intersection [19]. The stereo model set-up and the 3D stereo intersection are geometric issues. They use a CCRS developed parametric geometric model already tested on different data sets [20].

The images are SAR standard products generally available to users. They are generated digitally during post processing from the raw signal SAR data (Doppler frequency, time delay). Errors present in the input parameters to image geometry model will propagate through to the image data [21]. These include errors in the estimation of slant range and of Doppler frequency and also errors due to the satellite's ephemeris data and the ellipsoid. Assuming the presence of some geometric error residuals, the parameters of the geometric correction model using a rigorous parametric solution reflect these residuals. More details on the parametric solution for the CCRS geometric model can be found in [20] and its applicability to stereo images for DEM generation in [19].

The stereo model set-up is computed with an iterative least square bundle adjustment that enables the parameters of the geometric model to be refined with GCPs. The GCPs have to be acquired with stereo plotting [22] but tests with monoscopic plotting were also performed. The 3-D stereo intersection is performed using the previously computed geometric model to convert the pixel coordinates in both images determined in the image matching of the stereo pair to three-dimensional data. Cartographic coordinates (planimetry and height) in the user defined map projection system are determined for the measured point with a least-squares 3D-intersection process based on the geometric model equations and parameters [19].

The image matching is principally a radiometric issue. It can use computer-assisted (visual) or automatic methods. The computer-assisted or visual matching is done with the digital stereo workstation, the DVP, developed in collaboration between Laval University, Quebec, Canada, and CCRS. The system enables the on-line three-dimensional reconstruction of a stereo model and the capture in real time of planimetric and altimetric features [6], [19]. The stereoscopic viewing is related to conventional photogrammetric viewing with the split screen and a simple stereoscope. The control of image positioning follows the dynamic change to cancel the Y-parallax from the raw imagery, and retains real performance. In the same way as with a conventional stereo plotter, the operator cancels the X-parallax by fusing the floating marks (one per image) on the ground. It then measures the bidimensional parallax between the two images for each point. This visual operation then combines in the brain a geometric aspect (fusing the floating marks together) and a radiometric aspect (fusing the floating marks on the corresponding images point). That is the main advantage of the stereo viewing which improves the location of ground points and the extraction of information by integrating the simultaneous plotting, the general relief perception and the backscatter of both images [22], [23].

To evaluate the error of this processing step, two sub-areas of the study site were selected: one with low relief (slopes from 0º to 10º) , the other with medium relief (slopes from 10º to 30º). One thousand elevation points for each sub-area and each stereo configuration were extracted and directly compared with the 5-m accurate DEM derived from 10-m contour lines of the 1:50 000 topographic maps.

Most automated matching relies on correlation using different primitives (points, gradient, areas, semantic lists) to produce a disparity map [24]. The correlation can be done either by computing the maximum of a correlation coefficient, or by a least-square solution, which has been found to be the most accurate for VIR images [23]. An area correlation with the maximum of a correlation coefficient [25], a hierarchical least-square area correlation [26] or a multi-scale combined area/edge correlation [7] have been proved to be successful for SAR images. The solution chosen and adapted in the PCI digital image analysis system is a multiscale area correlation with the maximum of a normalized correlation coefficient [27]. This matching coefficient has been found the most accurate [28]. The number of steps involved in the multi-scale matching varies from five to eight with a maximum resolution reduction of 16. The correlation window size varies from eight "reduced" pixels at the coarsest resolution to 32 pixels at the full resolution.

To evaluate the error of this processing step, elevation points were extracted every two pixels on the full study site (4-5 000 000 points) and directly compared to the topographic DEM. The same sub-areas as before were also evaluated.

To summarize the stereo configurations as a function of the different parameters that are evaluated over the different slope relief (low and medium):

1. Fine mode (F) versus standard mode (S) or extended high (H) images;
2. Small (S4-S7) versus large intersection (S1-S7) angle:
3. Same side (F1-F5) versus opposite side (F4-F5) stereo;
4. Steep look (S1-S4) versus shallow look angles (S7-H6);
5. Speckle filtering or not of fine mode images (F4-F5);

V RESULTS AND DISCUSSION

Vb Stereo Model Set-Up

The first interesting result is related to the first part of this ADRO research on the localization accuracy of RADARSAT images: the GCPs acquisition method [22]. It is worthwhile to mention it, since it has an impact on the full processing. Plotting the GCPs in monoscopy for both images generates errors in the stereo model set-up two to four times larger than plotting them in stereoscopy. Since the monoscopic plotting on SAR images is about 1-2 pixels it generates an artificial parallax in the stereo model. True stereoscopic plotting enables a better relative correspondence of the GCP between the two images. Further results on the DEM errors will confirm the importance of acquiring GCPs with stereo plotting.

Sixteen stereo model set-ups were computed with stereo plotted GCPs. Fig. 6 shows the root mean square (RMS) residuals (in resolution unit) for the stereo pairs as a function of the intersection angle. The geometric error of the stereo model, as reflected by the RMS residuals, is reduced with a larger intersection angle. This is particularly noticeable between

4º and 23º with a plateau at 14º. The variations between the larger angles (89º to 101º) are not significant although more homogeneous due to the strongest geometry with opposite side stereo.

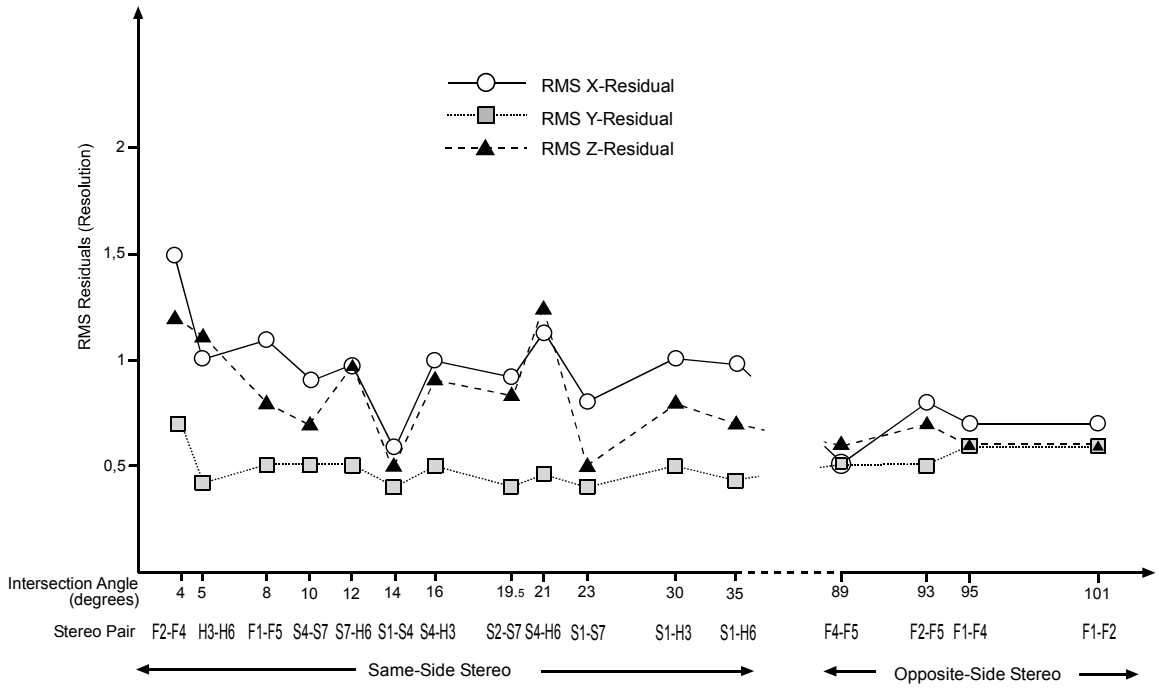

Figure 6: XYZ-Root mean square (RMS) residuals (in resolution unit) of the different stereo model set-up as a function of the intersection angle (in degrees). The GCPs have been stereo-plotted.

These results confirm the theoretical error propagation theory for the across-track (X) and elevation (Z) coordinates because the GCPs are well-defined targets in both images. The radiometry has thus a negligible impact on the error when compared to the geometry. For the along-track (Y) coordinate, which approximately corresponds to the satellite displacement, the variations are negligible since there is no squint angle for the RADARSAT-SAR [8], [21].

Vb Computer-Assisted Visual Matching DEM

Table II gives the general results for the computer-assisted visual matching DEMs extracted from nine different stereoscopic pairs. It gives the LE90 (elevation error with 90% of confidence), the bias, the minimum and maximum values in meters for the low and moderate relief. The last two are the same opposite-side stereo pairs (89° intersection-angle) created from ascending (asc.) and descending (desc.) orbits. In addition, the last one was also radiometrically pre-processed with an adaptive speckle

filtering [29] to evaluate the impact of the radiometric disparity reduction for this specific stereo configuration (both largest parallax and radiometric differences).

Table II: Characteristics of the stereo pairs and error results of the computer-assisted visual matching extracted DEM. Stereo pairs in italic are an opposite-side configuration.

Stereo pair	**Look angles**	**Intersection angle**	**Vertical Parallax Ratio**	**Type of relief**	**LE90 90%**	**Bias**	**Minimum Values**	**Maximum Values**
F1 asc.	37° – 40°	8°	0.30	**Low**	**21m**	**-7.2m**	**-44.6m**	**42.6m**
F5 asc.	45° – 48°			Moderate	39m	-5.5m	-78.5m	70.7m
S4 desc	34° – 40°	10°	0.39	**Low**	**24m**	**7.8m**	**-36.4m**	**53.8m**
S7 desc.	45° – 49°			Moderate	35m	1.4m	-58.8m	74.9m
S7 desc.	45° – 49°	11°	0.32	**Low**	**26m**	**-1.4m**	**-49.1m**	**46.6m**
H6 desc.	57° – 59°			Moderate	42m	8.6m	-78.8m	86.1m
S1 desc.	20° – 27°	13°	0.97	**Low**	**20m**	**3.4m**	**-48.7m**	**51.3m**
S4 desc.	34° – 40°			Moderate	37m	11.7m	-43.0m	82.2m
S4 desc.	34° –40°	15°	0.59	**Low**	**23m**	**2.3m**	**-32.9m**	**45.3m**
H3 desc.	51° - 55°			Moderate	37m	0.4m	-69.1m	74.4m
S7 asc.	45° – 49°	19°	0.99	**Low**	**21m**	**-2.4m**	**-40.5m**	**36.4m**
S2 asc.	24° – 31°			Moderate	41m	6.3m	-94.5m	69.9m
S1 desc.	20° – 27°	22°	1.37	**Low**	**22m**	**6.9m**	**-36.9m**	**56.9m**
S7 desc.	45° – 49°			Moderate	41m	9.3m	-68.2m	88.6m
F4 desc.	*43° – 46°*	*89°*	*1.97*	**Low**	**12m**	**-5.6m**	**-27.7m**	**21.8m**
F5 asc.	*45° – 48°*			Moderate	47m	11.7m	-66.1m	109.7m
F4 filter	*43° – 46°*	*89°*	*1.97*	**Low**	**14m**	**-7.8m**	**-30.0m**	**28.1m**
F5 filter	*45° – 48°*			Moderate	44m	6.6m	-97.0m	114.3m

Table II shows that there is no correlation between the intersection angle (or the VPR) and the LE90 results for the low or moderate relief sites. The principal parameter that has a significant impact on the precision of the DEM is the type of relief: with same side stereo pair, 20-26 m versus 35-42 m for the low versus moderate relief, respectively. Since the computer-assisted visual matching combines geometric and radiometric issues, the geometric advantages of a stereo pair are offset by its radiometric disadvantages, and vice versa; the rationale for each stereo pair is summarized below:

1. The greater the variation between two look angles (S1-S7) when compared to S1-S4 or S4-S7, the more the quality of the stereoscopic fusion deteriorated (21 m versus 20 m and 24 m, respectively). This cancels out the advantage obtained from the larger vertical parallax ratio.
2. The opposite-side stereo pair F4-F5 gives the best results (12 m versus 20-26 m) only for low relief (few radiometric disparities). Larger radiometric disparities for moderate relief cancel out its geometric advantages (47 m versus 35-42 m);
3. Steep stereo pair S1-S4 with a larger vertical parallax ratio than shallow stereo pairs S4-S7 or S7-H6 with better visual radiometry does not provide significantly better results (20 m versus 21 m or 26 m, respectively). It should be noted that these three stereo pairs have approximately the same intersection angle (10-13º);

4. Although a higher resolution, F1-F5, produced a better quality stereo pair when compared to S4-S7, it did not change the precision of the stereoscopic plotting for a given configuration (8°-10°-intersection angle with shallow look angles). The results are not better (21 m versus 24 m) in relation to the resolution ratio (7-9 m for fine mode versus 20-26 m for standard mode). Furthermore, although the speckle does not degrade the stereoscopic viewing, it does sometimes create confusion in the stereo plotting which also has an impact on the extreme values; and
5. The speckle filtering, by slightly reducing the image contrast, smoothes the low relief to decrease the accuracy (14 m versus 12 m), but reduces the larger radiometric disparities in the moderate relief to improve the results (42 m versus 47 m).

Vc Automatic Image Matching DEM

The first comparison is to verify the error propagation of the GCP collection methods as mentioned previously. The LE90 results for the entire DEMs extracted from only two stereo pairs (F5-F1 and S1-S7) gives:

- F5-F1: 30 m for the monoscopic plotting and 25 m for the stereoscopic plotting;
- S1-S7: 24 m for the monoscopic plotting and 14 m for the stereoscopic plotting.

The improvement for both images is in the same order relative to the resolution (7-9 m for fine mode versus 20-26 m for standard mode) and the plotting accuracy. It thus confirms the importance of the GCP collection with stereoscopic viewing to avoid the error propagation of artificial parallaxes of the GCP image coordinates.

Table III gives the general results for automatic image matching DEMs extracted from the nine different stereoscopic pairs. It gives the same statistical parameters as Table II. The LE90 are not as homogeneous as previously. Due to the moderate relief study site the radiometric issue is the main factor involved in the automatic image matching for the computation of the maximum correlation coefficient. Over rugged terrain the selection of the stereo pair should minimize the geometric differences between the two images (mainly the scale factor). The time separation in the acquisition of the two images, which is not an important issue with VIR images, is also a source of radiometric differences due to potential changes in the SAR and surface interaction (such as vegetation and soil properties) [30]. Consequently, automatic matching is more sensitive to radiometric disparities than visual matching. The geometric advantage can thus no longer compensate for the cumulative radiometric disadvantages during the matching, such as in the computer-assisted visual matching.

The relief is no longer the principal parameter that has an impact on the DEM accuracy such as in the computer-assisted visual matching. Large radiometric disparities in the stereo pair depending on different criteria related to the look angle (foreshortening, moisture, roughness, vegetation, etc.) and to the acquisition time difference should then account for the DEM accuracy. For example, in S4-H3 and S7-H6 stereo pairs comparisons the H3 and H6 images display more radiometric variations since the

vegetation component tends to dominate the return signal [30] and in addition, the H6 (12 January 1997) low signal returns from the frozen agricultural fields (Fig. 4). In the same way S2-S7 stereo pair displays foreshortening for S2 and not for S7 in the moderate relief.

Table III: Error results of the automatic image matching extracted DEM. Stereo pairs in italic are an opposite-side configuration.

Stereo Pair	**Vertical Parallax Ratio**	**Type of Relief**	**LE90 90% Confidence**	**Bias**	**Minimum Value**	**Maximum Value**
F2-F4 Same side	0.15	**Low**	**24 m**	**-4.5 m**	**-51.2 m**	**58.2 m**
		Moderate	*27 m*	*11.8 m*	*-36.2 m*	*90.0 m*
		Entire DEM	33 m	-7.3 m	-178.9 m	125.0 m
F5-F1 Same side	0.30	**Low**	**12 m**	**-13.3 m**	**-33.2 m**	**8.4 m**
		Moderate	*36 m*	*4.2 m*	*-39.6 m*	*95.0 m*
		Entire DEM	25 m	-1.1 m	-89.1 m	95.0 m
S7-H6 Same side	0.32	**Low**	**31 m**	**-50.4 m**	**-99.4 m**	**12.5 m**
		Moderate	*22 m*	*-57.5 m*	*-106.0 m*	*-6.0 m*
		Entire DEM	56 m	-76.3 m	-221.5 m	62.0 m
S4-S7 Same side	0.39	**Low**	**24 m**	**25.8 m**	**-16.1 m**	**58.6 m**
		Moderate	*46 m*	*-6.5 m*	*-81.2 m*	*42.6 m*
		Entire DEM	45 m	-1.3 m	-126.0 m	150.3 m
S4-H3 Same side	0.59	**Low**	**23 m**	**11.7 m**	**-101.7 m**	**42.0 m**
		Moderate	*59 m*	*-18.0 m*	*-116.6 m*	*42.0 m*
		Entire DEM	54 m	-21.9 m	-161.8 m	82.0 m
S1-S4 Same side	0.97	**Low**	**15 m**	**-17.1 m**	**-40.2 m**	**16.2 m**
		Moderate	*29 m*	*10.9 m*	*-23.0 m*	*66.6 m*
		Entire DEM	23 m	-11.9 m	-81.0 m	82.0 m
S2-S7 Same side	0.99	**Low**	**16 m**	**-19.3 m**	**-44.2 m**	**13.0 m**
		Moderate	43 m	-2.0 m	-64.7 m	61.0 m
		Entire DEM	39 m	-33.9 m	-148.7 m	61.0 m
S1-S7 Same side	1.37	**Low**	**11 m**	**-3.7 m**	**-22.0 m**	**25.3 m**
		Moderate	*27 m*	*6.6 m*	*-32.0 m*	*65.6 m*
		Entire DEM	14 m	-5.0 m	-61.0 m	71.3 m
F4-F5 Opposite side	*1.97*	**Low**	**16 m**	**-15.0 m**	**-108.6 m**	**19.1 m**
		Moderate	*107 m*	*-7.4 m*	*-179.0 m*	*199.0 m*
		Entire DEM	34 m	-11.8 m	-312.7 m	199.0 m
F4-F5 Opp. side Filtered	*1.97*	**Low**	**21 m**	**-17.4 m**	**-52.4 m**	**36.8 m**
		Moderate	*77 m*	*-2.2 m*	*-132.2 m*	*132.8 m*
		Entire DEM	47 m	-14.3 m	-289.5 m	260.1 m

Conversely, the "equivalent" radiometric relief-induced disparities for S1-S7 did not adversely affect the image matching. One potential reason of the high percentage of good matched points could be the close acquisition dates (24 and 22 October 1996), as mentioned previously, which have reduced the radiometric disparities due to SAR and surface interaction (such as vegetation and soil properties). Furthermore, the stronger geometry should not be the only parameter to explain these best results (LE90, bias and min/max values) since the entire DEM LE90 error decrease (64%) between S2-S7 and

S1-S7 is higher than their VPR increase (38%). More examples with other acquisition dates could resolve this ambiguity.

However, two trends can be detected from the results for the three test areas (low, moderate and entire DEM):

1. With equivalent geometric disparities (same vertical parallax ratio) the best radiometric stereo pair gives better results (F5-F1 versus S7-H6; S1-S4 versus S2-S7; F4-F5 filtered versus F4-F5 in the moderate relief);
2. With equivalent radiometric disparities, the best stereo geometry gives better results (S1-S4 versus S4-S7; S1-S7 versus S2-S7; etc.).

For the opposite-side stereo pair, the same explanation as before applied: only the moderate relief results are improved with the speckle filtering.

Another trend of these results, when compared with those of the computer-assisted visual matching, is that they are slightly better, except when the radiometric disparities are large (S4-H3, F4-F5) for which the geometric advantage cannot compensate. In the computer-assisted visual matching, the stereo plotting is performed at the pixel accuracy (no zoom available), but in automatic matching the maximum of the correlation coefficient is interpolated from the different matched pixels. It then gives a sub-pixel plotting, which reduces the range error, E_r, and consequently the elevation error, E_h (1). The improvement is thus more pronounced with the strongest same-side stereo geometry S1-S7 (11 m and 27 m versus 22 m and 41 m for low and moderate relief, respectively).

Fig. 7 is a graphic representation of same-side stereo pair LE90 results, but in resolution unit. The theoretical error for each stereo pair computed from (1) with the range error, $E_{r,}$ equal to one resolution has been added. It can be noticed that:

1. The practical DEM errors are lower than the theoretical error, especially for low VPR or intersection angle (F5-F1; S7-H6);
2. The shape of the low relief curve is quite “similar or parallel” to the theoretical one, because the radiometric disparities have less impact in the image matching; and
3. The moderate and entire DEM curves do not well mimic the theoretical one, even if there is a trend towards reducing the DEM error as the VPR increases. The radiometric disparities in the stereo pairs, S4-H3 and S2-S7, account for the variations to the theoretical curve.

These statements confirm that the theoretical error propagation modeling is not a good indicator by itself for predicting radargrammetric DEM accuracy, since it is only computed from the SAR geometric aspects. It should be combined with the VPR and the radiometric characteristics and disparities of the stereo pair, taking into account the different criteria of the SAR signal return.

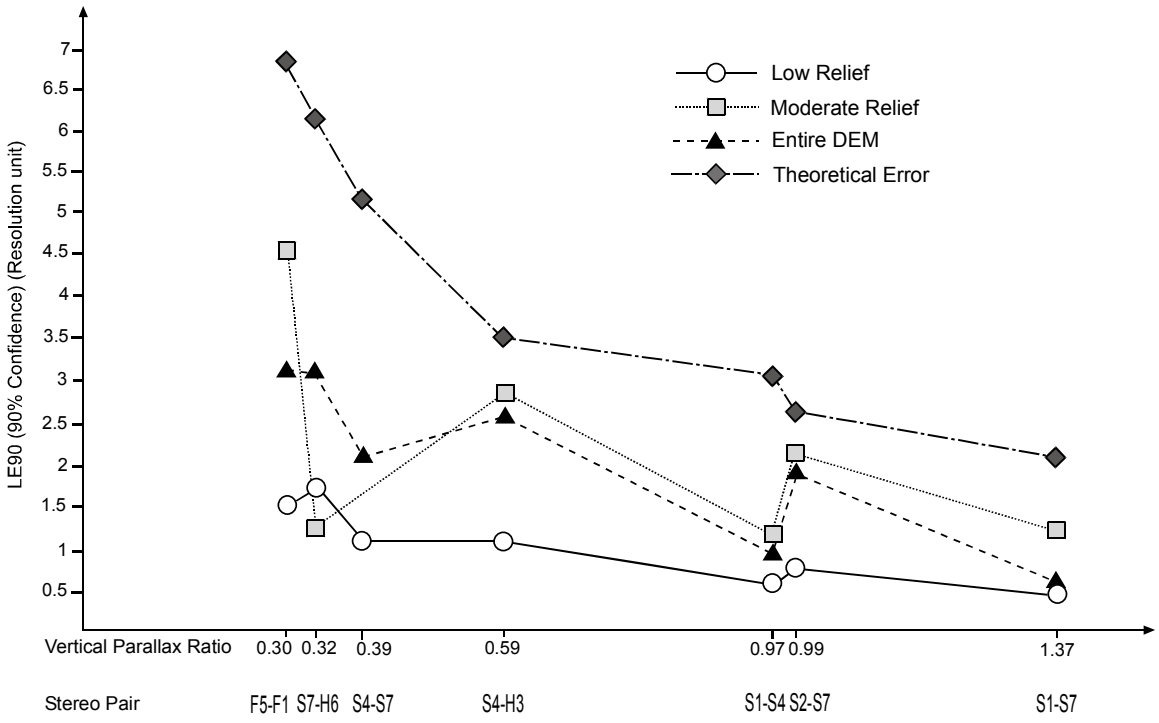

Figure 7: DEM accuracies (in resolution unit) of the different stereo pairs for the three test relief areas as a function of the vertical parallax ratio. The GCPs have been stereo-plotted. The theoretical error prediction curve, as computed from (1), is also added.

VI CONCLUSIONS

Previous research studies have shown a contradiction between the theoretical error propagation modeling and practical experiments, mainly in high relief areas. The error modeling accounts only for SAR geometric aspects, and not for radiometric ones. To resolve this contradiction the error propagation is tracked along the DEM generation processing steps (stereo model set-up, image matching, 3D intersection) using various RADARSAT stereo configurations of the Sherbrooke, Canada study site. After the stereo model set-up, elevation points were extracted with two matching processes (computer-assisted visual plotting and a multi-scale area correlation with the maximum of a correlation coefficient) and directly compared with an accurate topographic derived DEM.

The first results show that the stereo model set-up accuracy is correlated with the intersection angle in accordance with the theoretical error modeling, because the radiometry is not an important issue in the error propagation for the well-defined GCPs in both images. Previous experiments with the same data set showed that GCP selection with stereoscopic plotting increases this accuracy. It was confirmed that the monoscopic GCP plotting error propagates through the entire processing steps when comparing the final accuracy of the DEM generated from mono versus stereo plotting methods.

The computer-assisted visual matching results showed that the main parameter, which has an impact on DEM accuracy, is the type of relief: 20-25 m versus 35-42 m for low and moderate relief areas respectively, whatever the same-side stereo configuration. Only opposite-side stereo configuration achieved better results in low relief areas (12 m). Since both radiometric and geometric issues are involved in the computer-assisted visual matching, the advantage of one can compensate for the disadvantage of the other, and vice versa. Consequently, it is strongly recommended that the DEM accuracy be ascribed values that reflect the different areas of relief.

The automatic image matching results were slightly better in general (less than two resolution cells) due mainly to a sub-pixel matching. In flat relief, it is improved up to one resolution cell. When the radiometric disparities were too large (S4-H3, F4-F5), results were inverted since the geometric advantage (not involved in the automatic matching) cannot compensate for the radiometric disadvantage. On the other hand, the largest radiometric disparities with the large intersection-angle same-side stereo pair S1-S7 do not disturb the matching for the entire DEM, which consequently achieve good results with a stronger geometry. The potential reason could be the close acquisition date between the two images, which have reduced the radiometric differences of the vegetation and soil SAR backscatter.

Finally the comparison with the theoretical error propagation model shows better results for our experiment. Furthermore, the low relief DEM results curve as a function of the VPR is more in accordance with the theoretical prediction curve because the radiometric disparities have less impact than the geometric disparities in this type of relief. For the other relief the variations result from the specific radiometric disparities of the SAR signal return (not only induced by the relief) for each stereo pair.

The comparison of the two matching algorithms over low and moderate relief sub-areas has shown they are complementary, mainly when the radiometric disparities are large. The automatic image matching can be used for the first step of the DEM generation, and the computer-assisted visual matching in a second step to correct or edit the elevation points when the radiometric disparities are too large, and generate mismatch or no-match in the first step.

For wide separation of look angles, better stereo geometry is offset by poorer image fusion in the stereo viewing or matching. This implies that a tradeoff in the choice of the "better" stereo pair has to be reached for the reduction of either the geometric or the radiometric disparities, and there can be multiple solutions over the same study site. The tradeoff must first take into account the terrain since the relief is an important parameter in the final accuracy. The tradeoff has then to consider the radiometric characteristics and disparities of the stereo pair taking into account the SAR and surface interaction (surface geometry, vegetation, soil properties, geographic conditions, etc.) and the acquisition time separation. Geometric versus radiometric disparities and tradeoffs and general guidelines

are finally drawn in Table IV for selecting RADARSAT stereo pairs for DEM generation as a function of the terrain relief.

Table IV: Geometric versus radiometric disparity tradeoffs and general guidelines for selecting RADARSAT stereo pairs for DEM generation as a function of terrain relief.

Terrain Relief Slopes	**Flat 0° - 10°**	**Rolling 10° - 30°**	**Mountainous 30° - 50°**
Radiometric Disparities	Small	Medium	Large
Geometric Disparities	Large	Medium	Small
Trade-off	Opposite-side with steep look angles	Same-side with large intersection angle *or* (Opposite-side with shallow look angles)	Same-side with small intersection angle and steep or shallow look angles
Stereo RADARSAT Configurations	S1desc-S1asc F1desc-F1asc	S1-S7 (desc or asc) F1-F5 (desc or asc) *or* (S7desc-S7asc F5desc-F5asc)	S1-S4 (desc or asc) S4-S7 (desc or asc) F1-F4 (desc or asc) F2-F5 (desc or asc)

It shows that the solution is not unique because most of the times the images are generally not only used for DEM generation. The projected application requirements of the DEM and the thematic use of the images are thus other elements in the tradeoff to be decided by the end user. For example, a cartographer would prefer in a mountainous relief the F2-F5 stereo pair if he also wants to extract cartogaphic features, such as the transportation networks. Conversely, a geoscientist would prefer on the same study site the S4-S7 stereo pair for a better geomorphologic interpretation over a wider area coverage.

ACKNOWLEDGMENTS

This research was undertaken at the Canada Centre for Remote Sensing and the RADARSAT-SAR images were acquired as part of the Applications Development and Research Opportunity (ADRO) program sponsored by the Canadian Space Agency. The author would like to thank R. Chénier of Consultants TGIS, Inc. for the data acquisition and the stereo processing. The RADARSAT images are a courtesy of the Canadian Space Agency under the ADRO program.

REFERENCES

[1] G. La Prade, "An analytical and experimental study of stereo for radar," P*hotogrammetric Eng.*, vol. 35, no. 2, pp. 294-300, March 1963.

[2] F. Leberl, W. Mayr, G. Domik and M. Kobrick, "SIR-B stereo-radargrammetry of Australia," *Int. J. Remote Sensing*, vol. 9, no. 5, pp. 997-1011, 1988.

[3] F. Leberl, G. Domik, H. Raggam, J. and M. Kobrick, "Radar stereomapping techniques and applications to SIR-B images of Mt Shasta," *IEEE Trans. Geosci. Remote Sensing,* vol. 24, no. 4, pp. 473-481, July 1986.

[4] R. Simard, F. Plourde and Th. Toutin, "Digital elevation modeling with stereo SIR-B image data," in *Proc.7th Int. Symp. Remote Sensing for Resources Development and Environmental Management, ISPRS Commission VII*, Enschede, The Netherlands, Aug. 25-29, 1986, pp. 161-166.

[5] Z.-G. Twu and I. Dowman, "Automatic height extraction from ERS-1 SAR imagery," *Int. Archives Photogrammetry Remote Sensing*, vol. 31 (B2), pp. 380-383, 1996.

[6] Th. Toutin, "Opposite-side ERS-1 SAR mapping over rolling topography," *IEEE Trans. Geosci. Remote Sensing,* vol. 34, no. 2, pp. 543-549, March 1996.

[7] L. Marinelli, Th., Toutin et I. J. Dowman, «Génération de MNT par radargrammétrie : état de l'art et perspectives,» *Bulletin Soc. Française Photogrammétrie Télédétection*, vol. 148, pp. 88-96, 1997-4.

[8] S. Parashar, E. Langham, J. McNally, and S. Ahmed, "RADARSAT mission requirements and concepts," *Canadian J. Remote Sensing,* vol. 18, no. 4, pp. 280-288, December 1993.

[9] CSA, Canadian Space Agency, "Bringing Radar Application Down to Earth", in *Proc. RADARSAT ADRO Symp.*, Montreal, P.Q., Canada, October 13-15, 1998, CD-ROM.

[10] V. Kaupp, L. Bridges, M. Pisaruk, H. MacDonald and W. Waite, "Simulation of spaceborne stereo radar imagery: experimental results," *IEEE Trans. Geosci. Remote Sensing,* vol. 21, no. 2, pp. 400-405, Mar. 1983.

[11] G. Domik, "Evaluation of radar stereo viewability by means of simulation techniques," in *IGARSS,* Paris, France, ESA-SP-215, 1984, pp. 623-646.

[12] L. Polidori and P. Armand, "On the use of SAR image simulation for the validation of relief mapping techniques," *EARSeL J. Advances in Remote Sensing*, vol. 4, no. 2, pp. 40-48, Mar. 1995.

[13] H. Raggam and A. Almer, "Assessment of the potential of JERS-1 for relief mapping using optical and SAR data," *Int. Archives Photogrammetry Remote Sensing*, vol. 23 (B4), pp. 671-676, 1996.

[14] Fullerton, J.K., F. Leberl and R.E. Marque, "Opposite-side SAR image processing for stereo viewing," *Photogrammetric Eng. Remote Sensing*, vol. 52, no. 9, pp. 1487-1498, Sept. 1986.

[15] G.H Rosenfield, “Stereo radar techniques,” *Photogrammetric Eng.*, vol. 34, pp. 586-594, 1968.

[16] La Prade, G.L. “Subjective considerations for stereo radar,” in *Proc. 36th Annual Meeting Am. Soc. Photogrammetry*, Washington DC, pp. 640-651, 1970, Mar. 1-6.

[17] F. Leberl, “Accuracy analysis of stereo side looking radar,” *Photogrammetric Eng. Remote Sensing*, vol. 45, no. 8, pp. 1083-1096, Aug. 1979.

[18] L. Polidori et Th. Toutin, «Cartographie du relief par imagerie radar : l’ état de l’ art» *Bulletin Soc. Franç. Photogrammétrie Télédétection*, vol. 152, pp. 12-23, 1998-3.

[19] Th. Toutin, “DEM generation with a photogrammetric approach: examples with VIR and SAR images,” *EARSeL J. Advances in Remote Sensing*, vol. 4, no. 2, pp. 110-117, Mar. 1995.

[20] Th. Toutin, “Multi-source data fusion with an integrated and unified geometric modeling,” *EARSeL J. Advances in Remote Sensing*, vol. 4, no. 2, pp. 118-129, Mar. 1995.

[21] N. Denyer, R.K. Raney and N. Shepperd, “The RADARSAT SAR data processing facility,” *Canadian J. Remote Sensing*, Vol. 19, no. 4, pp. 311-316, Dec. 1993.

[22] Th. Toutin, **“**Evaluation de la précision géométrique des images de RADARSAT,” *J. canadien de télédétection*, vol. 23, no. 1, pp.80-88, Mar. 1998.

[23] I. J. Dowman, H. Ebner and C. Heipke, “Overview of European developments in digital photogrammetric workstations,” *Photogrammetric Eng. Remote Sensing*, vol. 58, no. 1, pp. 51-56, Jan. 1992.

[24] J.S. Greenfeld, “An operator-based matching system,” *Photogrammetric Eng. Remote Sensing*, vol. 57, no. 8, pp. 1049-1055, Aug. 1991.

[25] S. Sylvander, D. Cousson et P. Gigord, «Etude des performances géométriques de Radarsat,» *Bulletin Soc. Franç. Photogrammétrie Télédétection*, vol. 148, pp. 57-65, 1997-4.

[26] I. J. Dowman, Z.-G. Twu and P.-H. Chen, “DEM generation from stereoscopic SAR data,” in *Proc. Int. Symp. GER’97: Geomatics in the Era of RADARSAT*, Ottawa, Ont., Canada, May 25-30, 1997, CD-ROM.

[27] *OrthoEngineRE and OrthoEngineRE 3D*, Reference Manual, PCI Enterprises, Inc., Richmond Hill, Ont., Canada, Version 6.2, March 1998.

[28] F. Leberl, K. Maurice, J.K. Thomas and M. Millot, "Automated radar image matching experiment," *ISPRS. J. Photogrammetry Remote Sensing*, vol. 49, no. 3, pp. 19-33, Feb. 1994.

[29] A. Lopes, E. Nezry, R. Touzi and H. Laur, "Structure detection and statistical adaptive speckle filtering in SAR images," *Int. J. Remote Sensing*, vol. 14, no. 9, pp. 1735-1758, June 1993.

[30] J. B. Boisvert, T. J. Pultz, R. J. Brown and B. Brisco, "Potential of synthetic aperture radar for large-scale soil moisture monitoring: a review," *Canadian J. Remote Sensing*, vol. 22, no. 1, pp. 2-13, Mar. 1995.